Charge diffusion and loss as a function of absorption depth in X-ray CCD

M. Kohno[a], K. Imanishi[a,1], A. Bamba[a,1], M. Tsujimoto[a,1],
H. Murakami[a,1], T. Tsuru[a], K. Koyama[a]

[a]Department of Physics, Kyoto University, Sakyo-ku, Kyoto, 606-8502, Japan.

ABSTRACT

We study the relation between diffusion and loss of charge produced in X-ray CCDs with the fitting method. We obtain the extent and the pulse height of each X-ray event in a CCD by a two-dimensional image-fitting the charge distribution of the event. For the monochromatic X-rays, we find that the event with small extent keeps all the charge produced, while that with larger extent than a certain value loses some part of the produced charge as a function of extent. The result suggests that the event with a small extent is produced by an X-ray absorbed in the depletion layer. On the other hand, the event with large extent corresponds to an X-ray absorbed in the field-free region. We develop two new methods which enable us to derive the relation between the extent of an event and the absorption depth. One is performed by illuminating well calibrated monochromatic X-ray source. The other is realized by using with two monochromatic X-rays and enables us to measure the thickness of the CCD depletion layer without calibrating absolute flux of the monochromatic X-rays.

Keywords: X-ray CCD, Calibration

1. INTRODUCTION

A Charge Coupled Device (CCD) camera has become a standard detector for X-ray astronomy, with the energy resolution of $\sim$ 130 eV at 5.9 keV (FWHM), the position resolution reaching $\sim$ 10 μm, time resolution of several seconds, and the sufficient quantum efficiency in 0.1–10 keV band. The new generation of X-ray observatories, *Chandra*, *XMM-Newton* and ASTRO-E II are all equipped with CCD cameras.

Since the CCD for X-ray astronomy is operated in the photon counting mode, the position and energy of each X-ray event are available. The charge cloud produced by an X-ray absorbed near the pixel boundary splits into several pixels. Thus, we obtain total amount of the charge produced by the X-ray from sum of the pulse heights of them. In the grade method, which was first applied to *ASCA* SIS, the pulse heights of the event center pixel and its surrounding pixels exceeding a certain threshold (the split threshold) are summed up. The event analysis in *Chandra* ACIS and the *XMM-Newton* EPIC are the modified version of the *ASCA* grade method. Although the grade method is simple and useful, it is not applicable to a CCD with a small pixel size and/or a thick depletion layer, because the X-ray absorbed deep inside the CCD produces an event with much larger extent than the pixel size. Thus, Murakami et al.[1] developed a new method of event analysis, "the fitting method".

In this method, we fit the 5×5 pixels surrounding the event center with a 2-Dimensional Gaussian model and obtain the volume and width in σ, which correspond to the produced charge and the extent of the event, respectively (Figure 1). By using the fitting method, we obtained the relation between the event absorption depth and the extent for three CCDs.

2. EXPERIMENTS

We use three types of front side illuminated p-type CCD cameras. One is the X-ray Imaging Spectrometer (XIS) onboard ASTRO-E. The others are CCDs named Deep1 and Deep2, and made from an epitaxial wafer, which are developed by Hamamatsu Photonics K.K. (HPK).[2] The XIS system has a shielded frame store region and is operated in the frame transfer mode. On the other hand, the HPK CCDs are operated in the full-frame transfer mode with the readout times of 13 sec. The specification of the CCDs are listed in Table 1.

Correspondence: Email: kohno@cr.scphys.kyoto-u.ac.jp

[1] Research Fellow of the Japan Society for the Promotion of Science (JSPS)

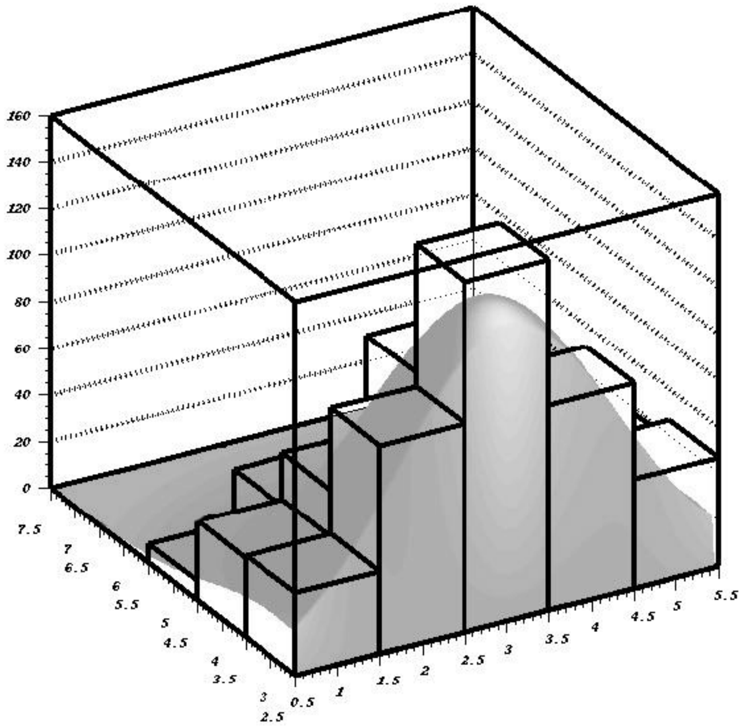

Figure 1. Image of the fitting method. The pulse heights of 5×5 pixels around event center are fitted by a two-dimensional Gaussian.

Table 1. Properties of CCDs

CCD	pixel size (μm)	number of pixel	readout noise (e^- r.m.s.)	thickness of wafer (μm)	back-diode
XIS	24×24	1024×1024	3	450	yes
Deep1	12×12	512×512	12	15	no
Deep2	12×12	512×512	12	50	no

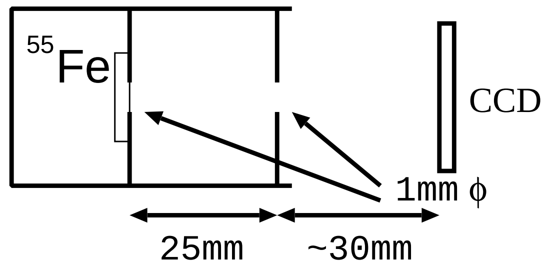

Figure 2. Radio isotope ^{55}Fe with collimators.

We use two kind of X-ray sources. One is a fluorescent X-ray generator, in which we used an X-ray tube from the KEVEX Corp. and secondary targets of iron (Kα: 6.40 keV, Kβ: 7.06 keV) and selenium (Kα: 11.22 keV, Kβ: 12.50 keV). The performance of this system is available in Ref. 3. Some uncertainties of the absolute fluxes from the X-ray generator remain. The other is a collimated Mn-K source shown in Figure 2, the flux from which can be fixed independent of the distance. We calibrated the absolute flux from the source with a proportional counter (1.1 photons sec^{-1}). We obtained data of HPK CCDs with both of the fluorescent X-ray generator and the collimated X-ray source. On the other hand, only fluorescent X-ray generator was used for XIS.

3. ANALYSIS AND RESULTS

3.1. Data Analysis

We extract events by following steps, which was developed to analyze data of XIS. First, we estimate the dark frame from the first 16 exposures. Second, we obtain the dark-subtracted frame data by subtracting the dark frame from each raw frame. Third, from the dark-subtracted frame data we pick up X-ray events, each of which contains a center pixel with a pulse height exceeding so-called "event threshold" and surrounding 5×5 pixels. The details of the procedure is given in Ref. 4. We, finally, obtain the pulse height and extent of each extracted event by applied the fitting method.

To study the diffusion and the recombination of electrons in a CCD, we plot the event extent (σ) against the event pulse height for each CCD with various X-ray energies (Figure 3). We call it "Ph-σ" diagram hearafter. Normalizing the pulse heights with the irradiated X-ray energy, we find that the event distribution in the Ph-σ diagram of each CCD has the same shapes among different X-ray energies. This result suggests that the relation between the event extent and charge loss rate is independent of the X-ray energies and determined only by the X-ray absorption depth. Since the rough shape of the Ph-σ diagram is same among all the CCDs we used, the diagram is commonly divided into two regions by the threshold shown with the dashed line in Figure 3. The event with larger extent than the threshold decreases the pulse height as the event extent increases, while the event with smaller extent than the threshold has almost the same pulse height.

Since the charge cloud produced in the depletion layers of a CCD drifts quickly toward the electrode, the extent of the charge cloud is small without the charge loss. While, the charge cloud produced in the field-free regions diffuses slowly and lose the charge by the recombination until reaching the boundary between the depletion layer and the field-free region. Thus, the charge cloud losing a part of the charge is largely extended under the electrode. Therefore, we conclude that the event with larger extent that the threshold are produced by an X-ray absorbed in the field-free region. On the other hand, the event below the threshold is from the X-ray absorbed in the depletion layer.

3.2. Extent and Depth

Following two methods shown below, we obtained the relation between the event extent and the X-ray absorption depth, assuming a increasing function between the event extent and the absorption depth, in other word, the event produced deeper inside a CCD is more extended.

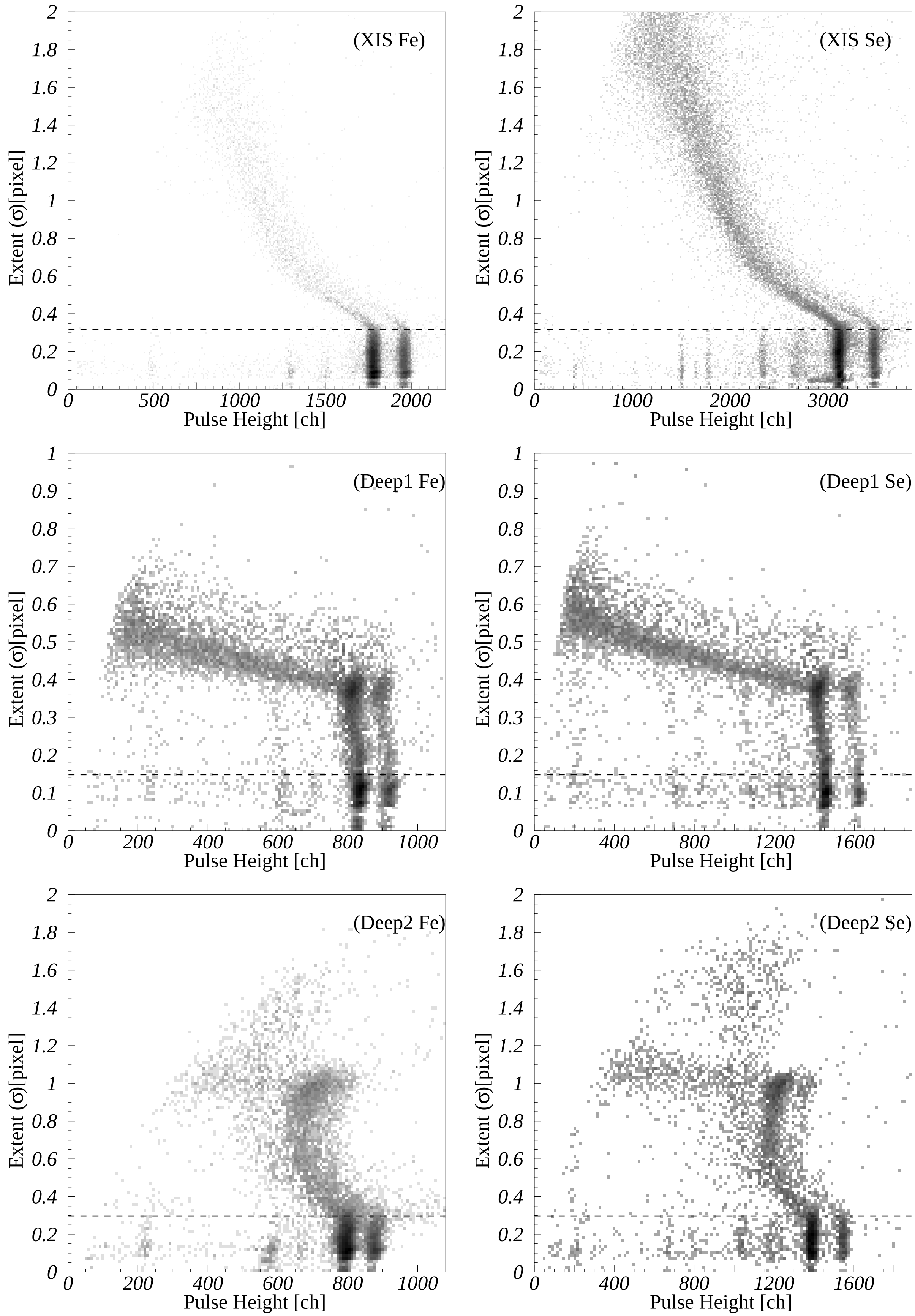

Figure 3. Plots of the pulse heights and event extents. From the upper panel, the data of XIS, Deep1, and Deep2. Left and right panels are the data of the fluorescent X-rays of Fe and Se, respectively.

3.2.1. Depth from Known Flux

We derive the relation from the data obtained with the collimated Mn-K X-ray source. Because, the X-ray flux is well calibrated, we can convert the event extent to the event absorption depth in the following procedure (see also Figure 4).

1. Count the events which have less extended than a certain value, and obtain the ratio to the total number of illuminated X-ray photons (Arrow 1 in Figure 4).
2. From the absorption coefficient of silicon, calculate the depth corresponding to the ratio (Arrow 2 and 3 in Figure 4).

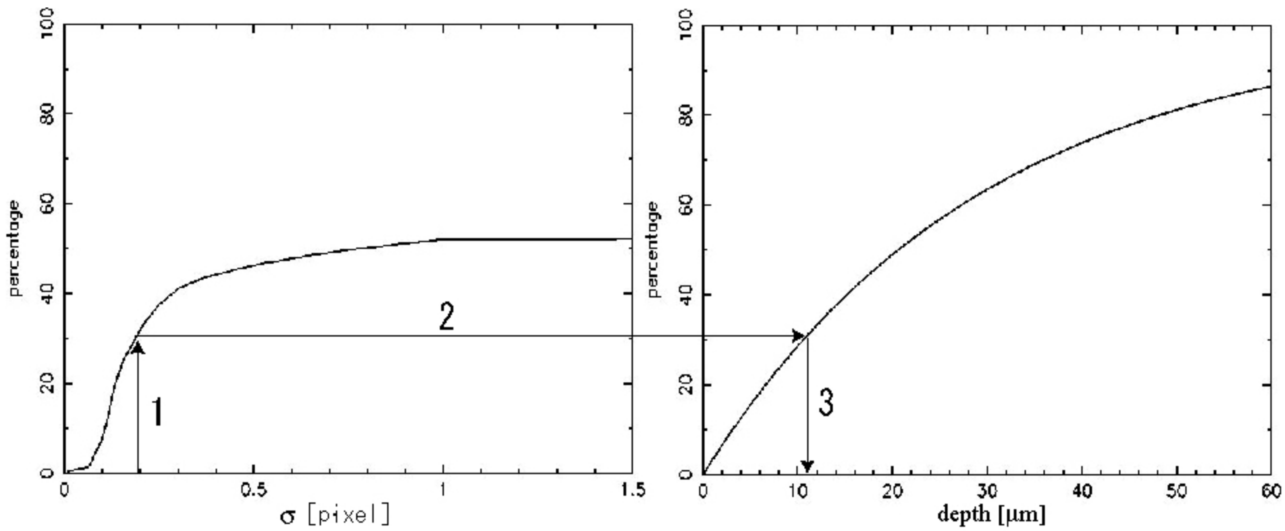

Figure 4. The illustration explaining the procedure to derive the event absorption depth corresponding to a certain event extent. The plot of the percentage of events have less extended than σ (results of the experiments: left panel), and the percentage of photons are absorbed less deeper than d (theory: right panel). We can convert a σ to a depth following the arrows.

The derived relation between the event absorption depth and the extent for Deep1 and Deep2 is given in Figure 5. We find that the relation changes at $\sigma \sim 0.15$ and 0.3 pixel in Deep1 and Deep2, respectively. This extent is equal to the beginning of the charge loss in Figure 3. Thus, we conclude that the event with a smaller extent than this threshold is from X-ray absorbed in the depletion layer. The extent of the X-ray event absorbed in the depletion layer is described by the equation?;

$$\sigma = \sqrt{\frac{2D\epsilon}{\mu q N_{\mathrm{A}}} \ln(\frac{x_d}{x_d - x})} \tag{1}$$

where D, ϵ, N_{A}, x_d, and x are the diffusion constant, the dielectric constant of silicon, the densities of acceptor, the thickness of the depletion layer, and the absorption depth. We fit this model to the data of Deep2 and get acceptable fit as in Figure 5.

3.2.2. Depth from X-rays with Two Energies

As shown in Section 3.1 and Figure 3, the comparison of the Ph-σ diagram obtained different illuminated X-ray energies suggests that X-rays absorbed in the same depth produce events with a same extent regardless of the X-ray energies. Thus, by utilizing that the absorption coefficient is dependent on X-ray energies, we can derive the relation between the event absorption depth and the event extent without calibrating the absolute X-ray fluxes, shown in the following manner.

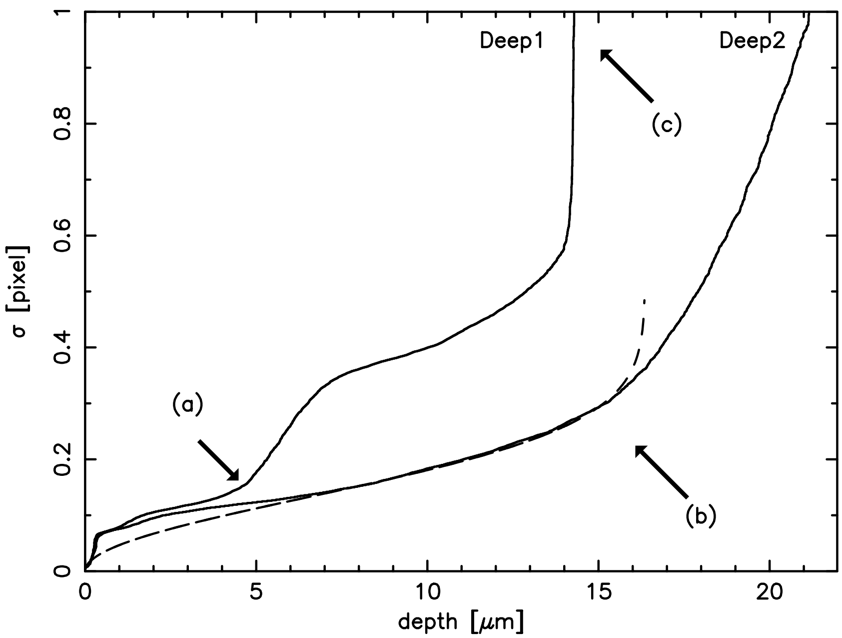

Figure 5. Relation between the event absorption depth and the event extent of Deep1 and Deep2. (a) and (b) correspond to the boundary of the depletion layer and the field-free region. (c) corresponds to the end of the epitaxial layer. The dashed line is the model for events absorbed in the depletion layer, fitted to the data of Deep2.

1. Make a plot of σ against $N(<\sigma)$ for two different X-ray energies, where $N(<\sigma)$ is number of events whose extents are less than σ (Figure 6).

2. Select two values of σ and make four equations like below.

$$\begin{aligned}
N_{\rm Fe}(<\sigma_1) &= N_{\rm Fe}\times(1-\exp(-\mu_{\rm Fe}\rho d(\sigma_1))) \\
N_{\rm Fe}(<\sigma_2) &= N_{\rm Fe}\times(1-\exp(-\mu_{\rm Fe}\rho d(\sigma_2))) \\
N_{\rm Se}(<\sigma_1) &= N_{\rm Se}\times(1-\exp(-\mu_{\rm Se}\rho d(\sigma_1))) \\
N_{\rm Se}(<\sigma_2) &= N_{\rm Se}\times(1-\exp(-\mu_{\rm Se}\rho d(\sigma_2)))
\end{aligned}$$

   Where, N, μ, and ρ, $d(\sigma)$ are the number of illuminated X-ray photons, the mass absorption coefficient of silicon, the density of silicon, and the depth corresponds to σ. Note that $d(\sigma)$ should be same between the two X-ray energies.

3. Solve the simultaneous equations, where unknown parameters are two $N_{E_{\rm X}}$ and two $d(\sigma)$.

This method is not suitable for thin devices, like Deep1, because the event absorption depth is small compared to the attenuation length of X-rays. Thus, we apply this method to the data of XIS and Deep2.

The plots of the event extent against the $N(<\sigma)$ are Figure 5. To avoid propagating the error of the event extents to the number of the events, we select two σ where the slope is large, as in Table 2. The calculated depth are also listed in Table 2.

For the confirmation of the derived relation, we obtained the relation between the event absorption depth and the extent for zinc-K X-rays. Figure 7 shows the relation for zinc-K X-rays with iron- and selenium-K X-rays, which indicates that the relation are very close among the for the third X-ray energies. The result of XIS can be compared with the previous calibrations. We calculate the number of the injected photons for the data of ^{55}Fe from the result. Then, we apply the grade method to the data, and the quantum efficiency of XIS with the grade method is measured

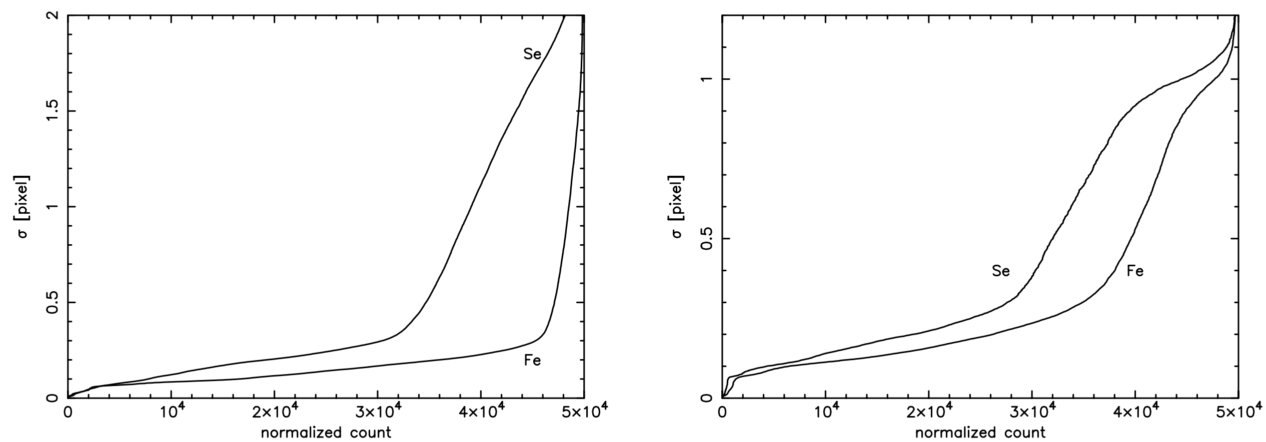

Figure 6. Plot of event extent to number of events small than that for XIS (left panel) and Deep2 (right panel). Counts are normalized as total counts become 50000.

Table 2. Parameters to derive the depth

CCD	σ_1 (pixel)	$N_{\rm Fe}(<\sigma_1)$	$N_{\rm Se}(<\sigma_1)$	σ_2 (pixel)	$N_{\rm Fe}(<\sigma_2)$	$N_{\rm Se}(<\sigma_2)$	$d(\sigma_2)$ (μm)
XIS	0.5	46610	33298	1.4	48072	37404	126
Deep2	0.3	14776	3720	0.9	19000	5321	37

to be 92% at 5.9 keV, which is consistent with the previous calibrations of 91%. However, we find the depths of events are large compared to the results of 3.2.1. This can occur if the flux of the collimated X-ray source is overestimate by 20%.

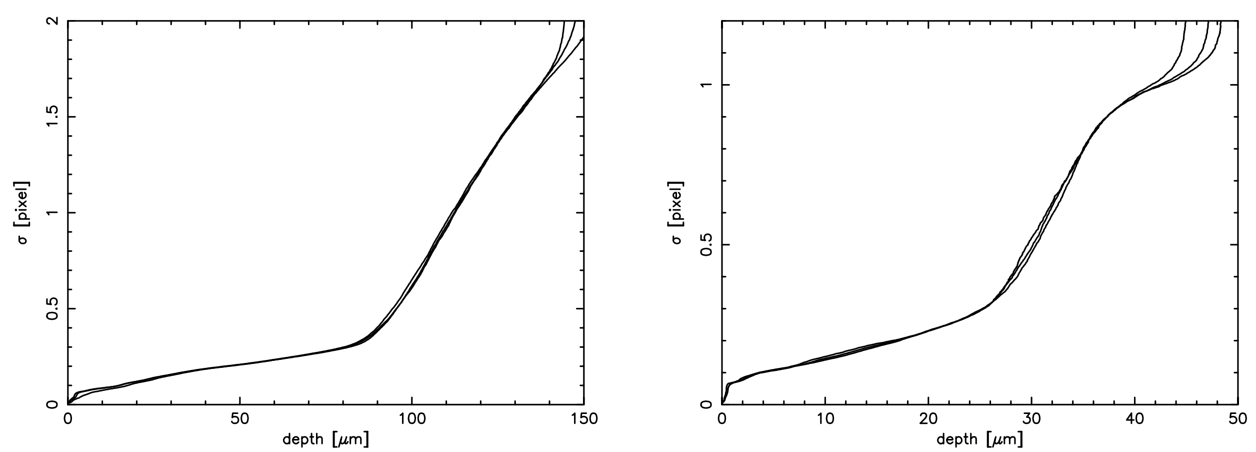

Figure 7. Plot of the relation between depth and extent for XIS (left panel) and Deep2 (right panel), derived from flux-unknown X-rays with two energies.

3.3. Charge Loss

The event produced in the field-free regions loses a part of the charge. Since Deep1 and Deep2 have a p+ layer below the field-free region, the charge cloud reaching the bottom of the field-free region is reflected toward depletion layer.

In the case of XIS, the charge cloud in the field-free region is drained out by the back-diode. Models of the charge loss rate as a function of the depth are given by Ref. 6. The model for Deep1 and Deep2 is;

$$Q(z) = \frac{\cosh(d/L - z/L)}{\cosh(d/L)}, \tag{2}$$

and for XIS is;

$$Q(z) = \frac{\sinh(d/L - z/L)}{\sinh(d/L)}, \tag{3}$$

where $Q(z)$, d, z, and L are the charge collection ratio, the thickness of the field-free region, the X-ray absorption depth from the boundary between the depletion layer and the field-free region, and the diffusion length of electrons. The fitted models are plotted in Figure 8. The diffusion length of an electron in the field-free regions is the free parameter, and is 60 μm, 24 μm, and 18 μm, for XIS, Deep1, and Deep2, respectively.

The event with the extent of $\sigma \sim 0.5$ (Deep1) and 1.1 (Deep2) loses large part of their charge. The event is produced near the bottom of the epitaxial layer, $d \sim 15$ μm and ~ 50 μm for Deep1 and Deep2, respectively (Table 1), where the lifetime of the electrons are shorter.

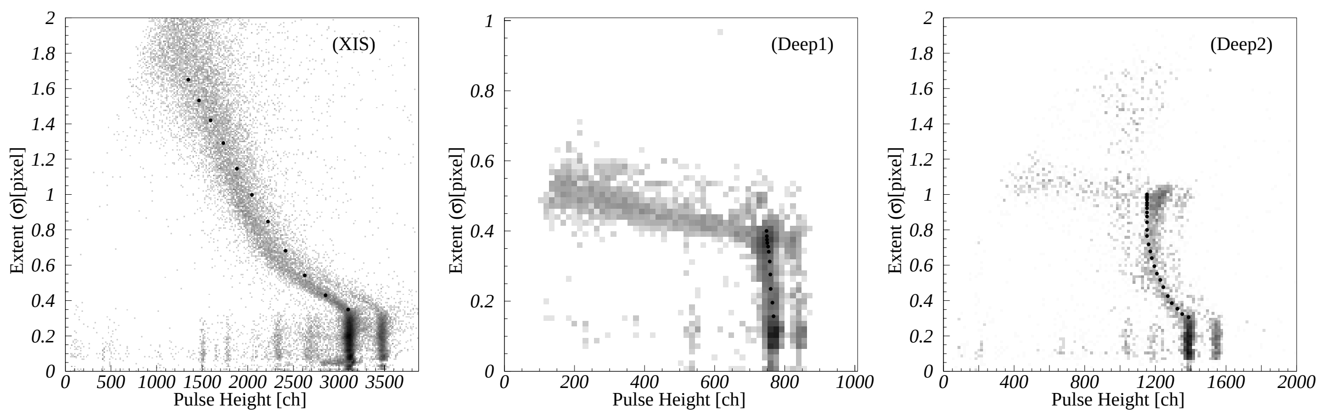

Figure 8. Plots of models of charge loss in field-free regions, from left XIS, Deep1, and Deep2. Dots represent models.

4. SUMMARY

We measure the event extent and charge loss rate of X-ray events. The Ph-σ diagram is divided into three regions shown in Figure 9. The events produced in the depletion layer have small extents and the same pulse height. While, the events from the field-free region have larger extents and lose some part of their charge. The third part, which is not seen in XIS, corresponds to the events produced near the bottom of the field-free region and they lose large part of their charge.

We successfully measure the relation between the extent of event and the X-ray absorption depth with the newly introduced two methods, one is the method in which the relation is obtained from a well calibrated X-ray source. In the other, we can derive it by illuminating without the information on the absolute fluxes of the calibrating X-ray sources. In other words, we showed that measurement of the quantum efficiency of a CCD can be made without absolute flux of X-ray calibration source.

acknowledgements

The authors express their thanks to all the member of the XIS team. K.I., A.B., M.T., and H.M. are financially supported by the Japan Society for the Promotion of Science.

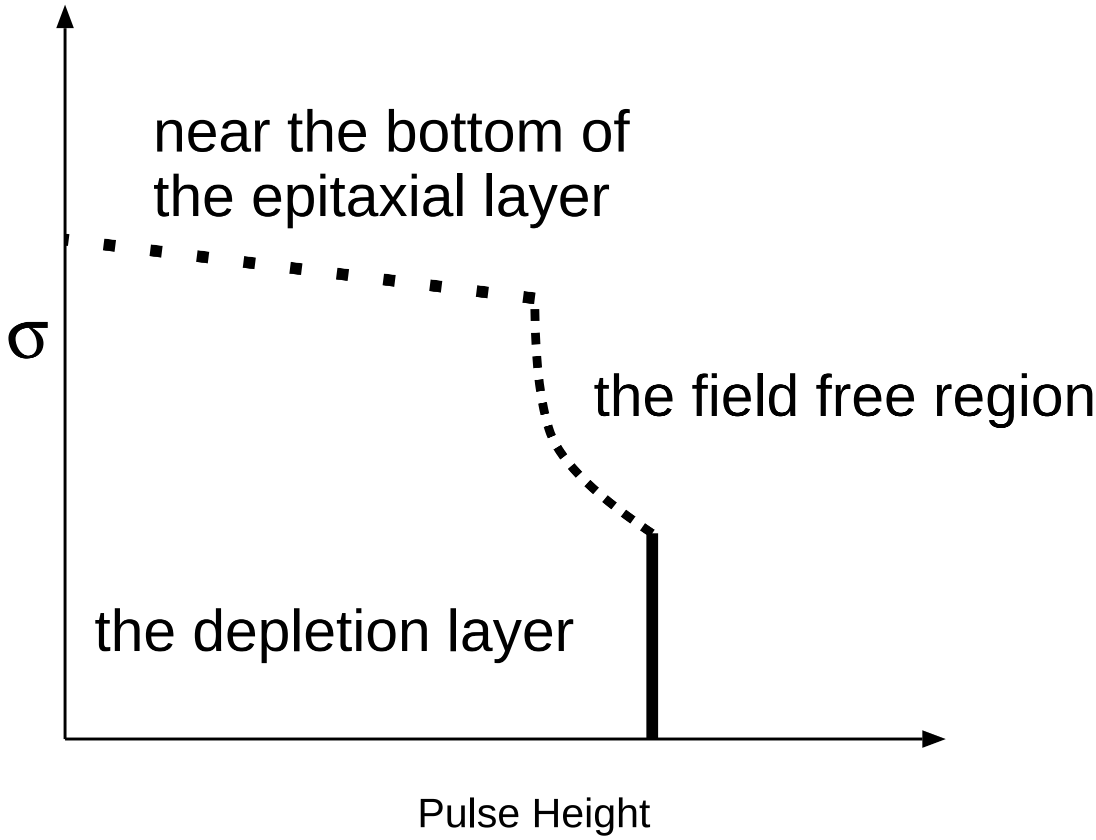

Figure 9. Schematic view of event distribution in pulse height - extent plane.

REFERENCES

1. Murakami H., et al. Proc SPIE, **3765**, 160, 1999
2. Miyaguchi, K. *Nucl. instr. and Meth.*, **436**, 24, 1999
3. Hamaguchi K., et al. *Nucl. Inst. and Meth.*, **450**, 360, 2000
4. Hayashida K. et al. Proc SPIE, **3445**, 278, 1998
5. S.M. Sze "Semiconductor devices: physics and technology", Wiley, New York, 1985
6. Hopkinson, G.R. *Nucl. Instr. and Meth.*, **216**, 423, 1983